Syntheses, Crystal Structures and Photophysical Measurements of Phosphite-Substituted Schiff Base and Azobenzene Ligands

Makeba B. Murphy-Jolly,*[a] Samuel B. Owens Jr. ,[a] Jason L. Freeman,[a] Gary M. Gray,*[a] Christopher M. Lawson,[b] and David P. Shelton[c]

Organic chromophores with charge asymmetry may exhibit significant second-order nonlinear optical (NLO) properties. Metal complexes have been used as the donor, the acceptor, or as the bridge in some of these chromophores. Metal complexes may also be useful in dipolar chromophore orientation and in the building of large molecular structures, but this approach remains largely unexplored. We herein report the syntheses and characterization of a novel class of phosphite-containing chromophores, O_2N-1-C_6H_4-4-CH=N-1-C_6H_4-4-$OP(OC_6H_4)_2$ (**2**) and O_2N-1-C_6H_4-4-X=N-1-C_6H_4-4-OP-$(OC_{10}H_6)_2$ [X = CH (**3**), N (**4**)], and their transition-metal complexes, *cis*-Mo(CO)$_4$(**2**)$_2$ (**5**), PdCl$_2$(**2**)$_2$ (**6**), and *cis*-Mo(CO)$_4$-

(**3**)$_2$ (**7**). The X-ray crystal structures of **2** and **5** show that coordination of the phosphite ligand to the metal atom does not alter the conformation of the chromophore. Hyper-Rayleigh scattering (HRS) measurements of the compounds in 1,4-dioxane at 1064 nm indicate that phosphite functionalization causes a small decrease in the β values of the Schiff-base chromophores {β [esu]: 47×10^{-30} (**1**), 25×10^{-30} (**2**), 30×10^{-30} (**3**)} and no change in the β value of the azo chromophore {β [esu]: 62×10^{-30} (**4**)}. The larger β values of the *cis*-Mo(CO)$_4$-L$_2$ complexes {β [esu]: 38×10^{-30} (**5**), 41×10^{-30} (**7**)} as compared to those of the ligands (**2** and **3**) are consistent with the 90° orientation of two chromophores in the complexes.

Introduction

Second-order NLO organic and organometallic materials have been found to be useful in computers, data storage, electro-optic modulation, medical imaging, and telecommunications.[1–8] Because the success of many of these applications depends on the strength of the second-order NLO material, there has been a significant effort to improve the performance of second-order NLO organic and organometallic materials by designing molecules with large first hyperpolarizibilities (β).[9–20] Many of the most promising second-order NLO materials are dipolar aromatic molecules possessing an electron donor and acceptor group, because larger second-order optical nonlinearities can arise from the intramolecular charge transfer between the opposite groups through their π-conjugated systems.[21–25] Organometallic and coordination metal complexes represent a growing class of second-order NLO compounds that offer additional flexibility and tunability.[26]

A potential and complementary approach to developing molecules with even stronger second-order NLO responses is to coordinate known organic chromophores such as (*E*)-stilbenes, diaryl Schiff bases, and azobenzene compounds that are known to have large β values to transition-metal centers. Orientations, which result in alignments of the dipoles in the complexes, should result in materials with even higher second-order NLO responses. We have initiated a project to synthesize phosphite-modified organic chromophores that can be easily attached to metal centers and to characterize the manner in which coordination to metal centers affects their β values. We herein report the synthesis of novel phosphite-substituted Schiff bases and azobenzenes and their respective transition-metal complexes. Coordination of the phosphite ligands to transition-metal centers allows the groups to be oriented in different manners relative to one another. The introduction of a binaphthyl-diyl phosphite group into some of these derivatives allows chiral materials to be prepared. The compounds have been fully characterized by elemental analyses, multinuclear NMR, and UV/Vis spectroscopy. Compounds **2** and **5** have been characterized by X-ray crystallography. The hyper-Rayleigh scattering (HRS) technique has been used to measure the β values of the ligands and complexes.

## Results and Discussion

Ligand Syntheses

The phosphite-substituted Schiff base and azobenzene ligands **2**, **3**, and **4** were synthesized in moderate to high

[a] Department of Chemistry, University of Alabama – Birmingham,
1530 Third Ave S., Birmingham, Alabama 35294-1170, USA
Fax: +1-205-934-2543
E-mail: mbmjolly@uab.edu
    gmgray@uab.edu
[b] Department of Physics, University of Alabama – Birmingham,
1530 Third Ave S., Birmingham, Alabama 35294-1170, USA
[c] Department of Physics and Astronomy, University of Nevada – Las Vegas,
4505 S. Maryland Parkway, Las Vegas, Nevada 89154-4002, USA

yields by using the procedure shown in Scheme 1. All of the reactions were relatively rapid. The synthesis of **2**, which has the smaller biphenyldiyl phosphite group, reached completion at ambient temperature after 1 h, and the syntheses of **3** and **4**, which have the larger binaphthyldiyl phosphite groups, reached completion at room temperature after 2 h. The ligands were purified by flash chromatography to avoid the significant product loss that occurs upon prolonged exposure to silica gel during traditional column chromatography. Ligand **2** was recrystallized by layering hexanes on a dichloromethane solution of **2** to give X-ray quality crystals. Attempts to obtain X-ray quality crystals of ligand **4** were unsuccessful.
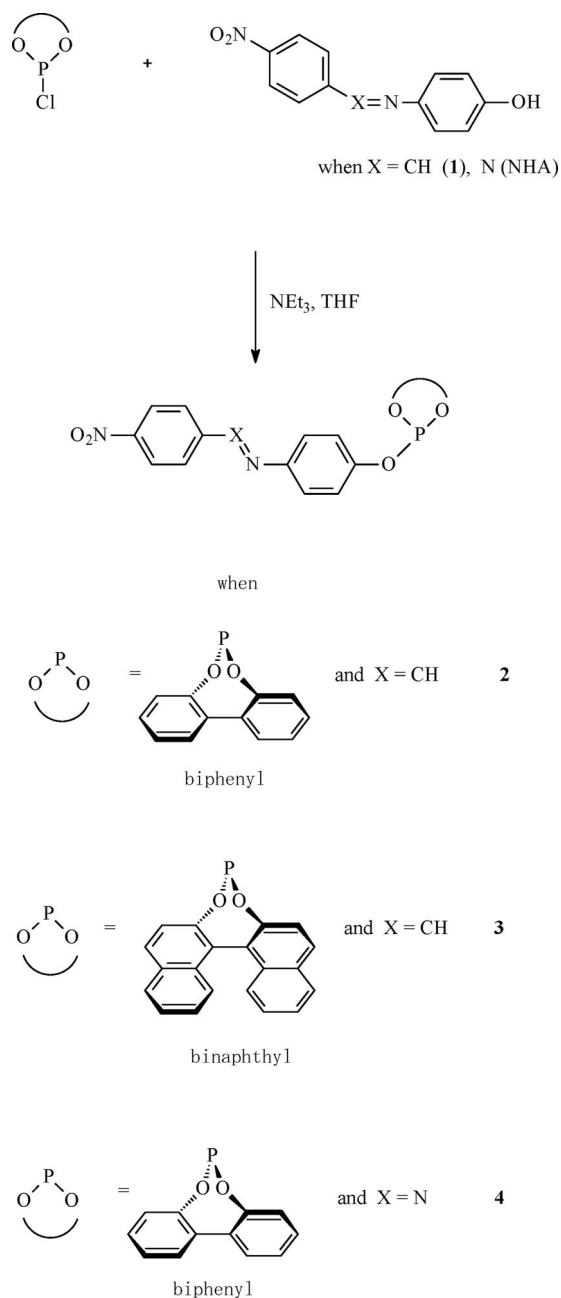
Scheme 1. Syntheses of phosphite-substituted Schiff base and azobenzene ligands **2–4**.

Of particular interest is the remarkable stability of these ligands. Ligand **2** did not show any changes in its ^{1}H and ^{31}P{^{1}H} NMR spectra even after six months of exposure to both air and water. This enhanced stability of the phosphites may be due to the D–π–A electronic system in the Schiff base and azobenzene moieties of the molecule that presumably reduces the availability of the lone pair of electrons on the phosphorus atom.

Complex Syntheses

The *cis*-Mo(CO)$_4$L$_2$ complexes **5** and **7** were synthesized by simultaneous additions of solutions of Mo(CO)$_4$(nbd) (nbd = 2,5-norbornadiene) and ligands **2** or **3**, respectively, in dichloromethane by syringe as shown in Scheme 2. Although both reactions were relatively rapid, steric hindrance due to the bulkier binaphthyl group slowed down the formation of **7**. The complexes were purified by fractional recrystallization by layering hexanes on saturated dichloromethane solutions of the complexes. This procedure gave X-ray quality crystals of **5**, but yielded **7** as a microcrystalline solid. The two diastereomers of **7** show sufficiently different solubilities so that they could be separated in this manner. Analytically pure samples of both complexes were obtained in moderate to good yields by this method.

The reaction of ligand **2** with PdCl$_2$(MeCN)$_2$ in MeCN, shown in Scheme 2, gave a quantitative yield of analytically pure **6**, which quickly precipitated from the solution. Complex **6** was insoluble in all common organic solvents except warm [D$_6$]DMSO. Attempts to form dichloropalladium(II) and dichloroplatinum(II) complexes of the more bulky binaphthyl ligands **3** and **4** were unsuccessful.

NMR Characterization of Ligands and Complexes

The ligands and complexes were characterized by using ^{1}H, ^{31}P{^{1}H}, and ^{13}C{^{1}H} NMR spectroscopy and elemental analyses. All characterization data are consistent with the expected structures and demonstrate the high purity of the ligands. The ^{1}H and ^{13}C{^{1}H} NMR resonances were partially assigned by using 2D heteronuclear multiple-bond correlation (HMBC) spectroscopy, ACD/Labs NMR prediction and simulation software, and the assignments for previously synthesized molecules with similar biphenyl and binaphthyl backbones.

X-ray Crystal Structures of 2 and 5

Crystals of ligand **2** and of its *cis*-Mo(CO)$_4$ complex **5** suitable for X-ray diffraction were obtained by slow diffusion of hexanes into concentrated dichloromethane solutions of the compounds. The molecular structures of **2** and **5** were determined and are shown in Figures 1 and 2, respectively. Both **2** and **5** crystallize in centrosymmetric monoclinic space groups ($P2_1/c$ for **2** and $P2_1/n$ for **5**).
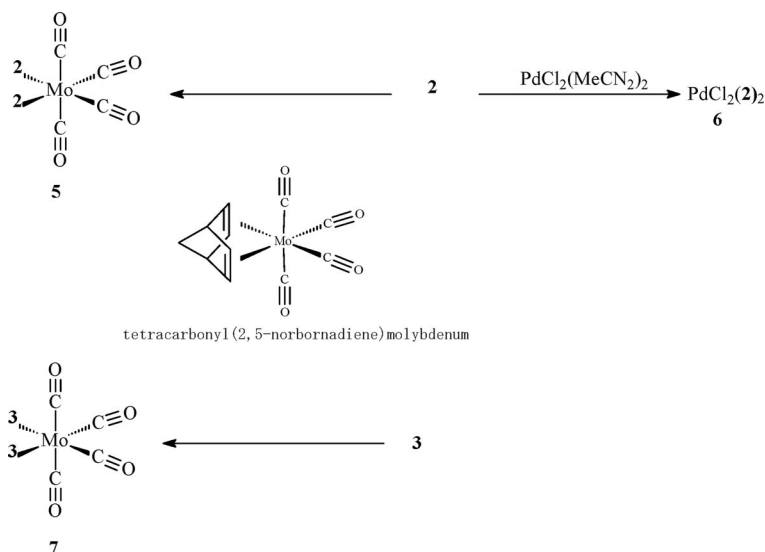
Scheme 2. Syntheses of transition-metal complexes of phosphite-substituted Schiff base and azobenzene ligands **5**–**7**.

Figure 1. ORTEP[39] plot of the molecular structure of compound **2**. Hydrogen atoms are omitted, and the atomic displacement ellipsoids are drawn at 25% probability.
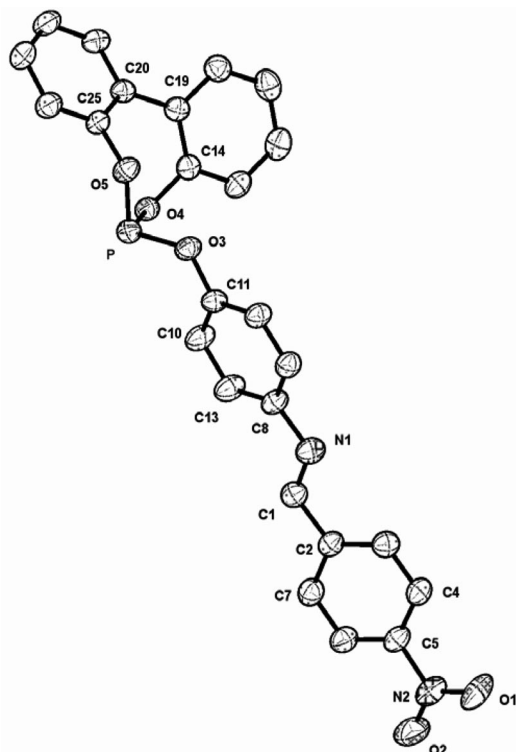

Figure 2. ORTEP[39] plot of the molecular structure of compound **5**. Hydrogen atoms are omitted, and the atomic displacement ellipsoids are drawn at 25% probability.

The most important conformational aspect of the structures of **2** and **5** is the relative planarity of the NLO chromophore in the compounds, because this could affect the aromaticity of the chromophore. The relative planarity of the chromophore is defined by rotations about the three bonds as measured by the torsion angles: (1) C13–C8–N1–C1, (2) N1–C1–C2–C7, and (3) C4–C5–N2–O1. As the data in Table 1 shows, major distortions from planarity in both
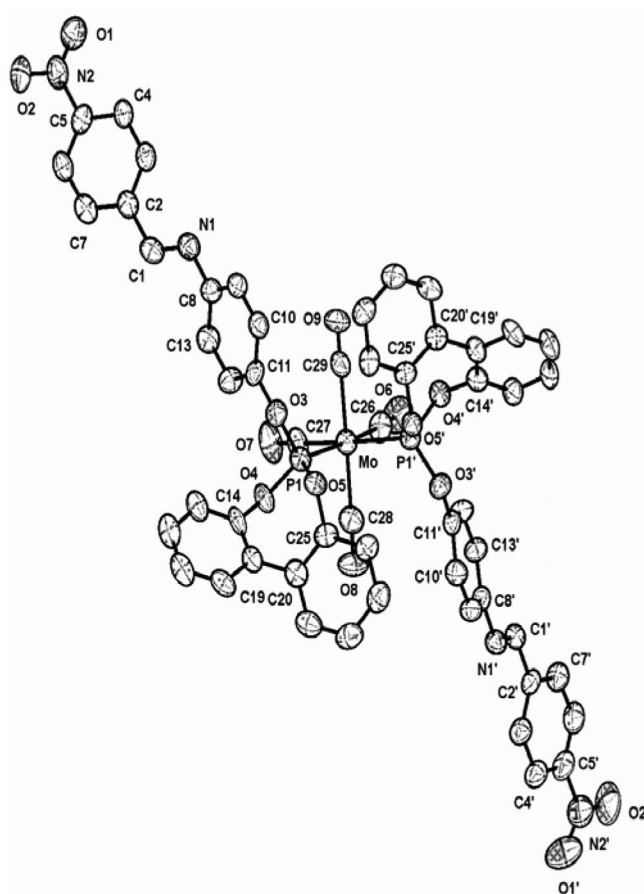
2 and **5** arise from rotations about the N1–C8 bonds [20.1(14) to 39.2(14)°]. There are also smaller rotations about the C5–N2 bonds in **5** [12(2) and 18.9(15)°] and about the C1–C2 bond in one of the ligands in **5** [169.4(9)°].

In contrast, the rotations about the C5–N2 and C1–C2 bonds in **2** are considerably smaller [C4–C5–N2–O1: 4.8(7)°; N1–C1–C2–C7: 178.4(4)°].

Table 1. Selected torsion angles [°] for **2** and **5** (**5L**/**5L′** represent the two ligands in complex **5**).

	2	**5L**	**5L′**
C10–C11–O3–P	–167.4(3)	–140.2(7)	–143.4(7)
C11–O3–P–O4	–81.2(3)	–78.9(7)	–83.9(7)
C11–O3–P–O5	177.3(3)	178.3(6)	174.7(4)
C13–C8–N1–C1	–23.6(7)	39.2(14)	20.1(14)
N1–C1–C2–C7	178.4(4)	–172.7(9)	–169.4(9)
C4–C5–N2–O1	4.8(7)	18.9(15)	12(2)
C14–C19–C20–C25	43.4(6)	43.3(13)	43.2(13)
C25–O5–P–O4	48.1(3)	52.6(7)	49.8(6)
C20–C25–O5–P	–77.2(4)	–74.6(9)	–75.7(9)
C14–O4–P–O5	43.8(3)	36.6(8)	41.9(6)
C19–C14–O4–P	–74.4(4)	–72.1(10)	–73.9(10)

Another interesting aspect of the structures of **2** and **5** is the conformation of the seven-membered dioxaphosphepin rings (**2**: P–O4–C14–C19–C20–C25–O5; **5L**: P1–O4–C14–C19–C20–C25–O5; **5L′**: P1′–O4′–C14′–C19′–C20′–C25′–O5′). This is best defined by the five torsion angles C14–C19–C20–C25, C25–O5–P–O4, C20–C25–O5–P, C14–O4–P–O5, and C19–C14–O4–P. The similarity of these angles in **2**, **5L**, and **5L′** suggests that coordination to the phosphorus atom does not significantly affect the conformation of the dioxaphosphepin ring. This is consistent with what has been previously observed for *cis*-Mo(CO)₄(2,2′-$C_{12}H_8O_2POCH_3$)₂, which has simpler phosphepin ligands,[27] and indicates that the phosphepin ring has a strongly preferred conformation that is not significantly affected by hydrogen bonding or crystal-packing forces.

The orientation of the chromophore relative to the phosphepin ring is also important. Given the rigidity of the phosphepin ring described in the previous paragraph, this is determined solely by rotations about the P–O3 and O3–C11 bonds. The rotation about the P–O3 bond as shown by the C11–O3–P–O4 and C11–O3–P–O5 torsion angles in Table 1 is nearly the same in both the free ligand **2** and in the two ligands in **5**. In contrast, the rotation about the O3–C11 bond as shown by the C10–C11–O3–P torsion angle changes significantly (an average of 25°) when the ligands are coordinated to the *cis*-Mo(CO)₄ center. This reduction in the C10–C11–O3–P torsion angle upon coordination appears to minimize the interaction between the adjacent ligands in the complex. In spite of the difference in the torsion angles, the chromophores are oriented to point away from the phosphepin groups in both the free ligand **2** and in the two ligands in **5**.

The final conformational aspect of interest is the coordination environment of the molybdenum atom in **5**, which is a slightly distorted octahedron. The P1′–Mo–P1 bite angle is slightly larger than 90°, which causes the C27–Mo–P1, C28–Mo–P1, C26–Mo–P1′, and C29–Mo–P1′ angles to be slightly less than 90°, as shown in Table 2. The molybdenum–carbonyl bond lengths in Table 3 show the expected trend[27,28] with the carbonyl groups *trans* to the phosphepin groups having slightly shorter Mo–C bond lengths than do the carbonyl groups *trans* to each other (difference ca. 2σ). This is consistent with the fact that phosphites are stronger σ-donors and weaker π-acceptors than their carbonyl counterparts. However, the expected longer C–O bonds of the ligands *trans* to ligand **2** were not observed, and this is likely due to the crystal-packing forces in the solid-state crystal structure.[29,30]

Table 2. Selected bond angles [°] for **2** and **5** (**5L**/**5L′** represent the two ligands in complex **5**).

	2	**5L**	**5L′**	**5**	
O5–P–O3	92.33(15)	91.5(3)	91.4(3)	P1′–Mo–P1	98.33(8)
O5–P–O4	100.70(15)	102.0(3)	100.7(3)	C27–Mo–P1	87.8(3)
O3–P–O4	102.35(15)	103.7(3)	103.4(3)	C26–Mo–P1	175.2(3)
C11–O3–P	122.6(3)	126.0(5)	127.2(6)	C28–Mo–P1	86.5(3)
C1–N1–C8	121.0(4)	121.2(9)	122.0(8)	C29–Mo–P1	92.3(3)
C6–C5–N2	119.5(4)	119.5(10)	119.1(14)	C26–Mo–P1′	86.3(3)
				C27–Mo–P1′	173.9(3)
				C28–Mo–P1′	91.2(3)
				C29–Mo–P1′	88.9(3)

Table 3. Selected bond lengths [Å] for **2** and **5** (**5L**/**5L′** represent the two ligands in complex **5**).

	2	**5L**	**5L′**	**5**	
O3–P	1.626(3)	1.611(6)	1.606(6)	P1–Mo	2.429(3)
O4–P	1.625(3)	1.617(6)	1.607(6)	P1′–Mo	2.428(2)
O5–P	1.620(3)	1.606(6)	1.636(5)	C26–Mo	2.018(11)
C11–O3	1.385(5)	1.396(10)	1.403(9)	C27–Mo	1.980(11)
C8–N1	1.432(5)	1.424(11)	1.443(10)	C28–Mo	2.028(11)
C1–N1	1.249(5)	1.258(11)	1.255(10)	C29–Mo	2.033(10)
C1–C2	1.465(6)	1.466(13)	1.471(12)	C26–O6	1.135(10)
C5–N2	1.465(6)	1.470(13)	1.491(16)	C27–O7	1.150(11)
N2–O1	1.211(6)	1.191(10)	1.200(17)	C28–O8	1.154(11)
N2–O2	1.214(5)	1.222(11)	1.216(15)	C29–O9	1.130(10)

Linear and Nonlinear Optical Characterization

The linear absorption of solutions of chromophores NHA and **1**, ligands **2**–**4** and the metal complexes **5** and **7** in 1,4-dioxane are summarized in Table 4. All the compounds show an absorption band between 340 and 380 nm. These bands undergo a hypsochromic shift with both phosphite functionalization of the precursor chromophore and complexation of the phosphite to the molybdenum center. Shoulders observed between 230 and 280 nm are due to the overlapping π→π* transitions of the biaryl moieties[31] and the chromophore.

The β values of solutions of **1**–**5** and **7** in 1,4-dioxane were measured by using the HRS technique. The HRS measurements were carried out at a laser wavelength of 1064 nm and a sample temperature of 25 °C. Calibration of the results of the HRS experiment requires a reference standard, and 4-nitroaniline was used for this purpose, because its second-order nonlinearity is well studied and has been described previously in great detail.[32–35] Table 4 summarizes the data obtained from the HRS measurements of these ligands.

Table 4. Linear and nonlinear measurements of compounds (NHA, **1–5**, and **7**).

Sample	λ_{max} [nm]	β/β_{pNA}[a]	β ($\times 10^{-30}$ esu)	I_{VV}/I_{HV}
*p*NA	354	1	21.3	4.8 ± 0.1
NHA	374	2.83 ± 0.10	60 ± 2	4.8 ± 0.1
1	377	2.20 ± 0.08	47 ± 2	4.8 ± 0.1
2	346	1.18 ± 0.05	25 ± 1	4.4 ± 0.2
3	356	1.42 ± 0.05	30 ± 1	4.4 ± 0.1
4	351	2.90 ± 0.10	62 ± 2	4.6 ± 0.1
5	359	1.78 ± 0.06	38 ± 1	4.6 ± 0.1
7	372	1.91 ± 0.07	41 ± 1	4.2 ± 0.1

[a] β = 2470 au for *p*NA in 1,4-dioxane at 1064 nm;[38] 1 au = 3.20636×10^{-53} C³mJ⁻² = 8.6392×10^{-33} esu = 3.6213×10^{-42} m⁴V⁻¹.

Many nonlinear optical chromophores exhibit significant two-photon fluorescence (2PF).[32,36] This has sometimes led to overestimation of the β values obtained from HRS measurements. Since the 2PF spectrum is typically much broader than the HRS spectrum, spectral measurements are the most reliable way to distinguish between HRS and 2PF.[32,36] In this work, the HRS signal is measured with two different detection bandwidths to assess possible 2PF contamination of the HRS signal. The 60 cm⁻¹ (1.6 nm) bandwidth includes the entire HRS spectrum but may also include significant 2PF. The 0.3 cm⁻¹ (0.01 nm) bandwidth effectively excludes 2PF but cannot be used alone since it cuts off the wings of the HRS spectrum. For *p*NA, 58% of the intensity of the entire HRS spectrum (measured with 60 cm⁻¹ bandwidth) falls within the 0.3 cm⁻¹ bandwidth. The fraction will be larger for all the other chromophores in this study since the slower reorientation of these larger molecules results in a narrower HRS spectrum. The measured fraction is in the range 74–85% for all the ligands except **4**, which indicates negligible 2PF contribution to the signal. The fraction for ligand **4** is 62%, which indicates that 2PF contributes 15% ± 5% of the signal measured with 60 cm⁻¹ bandwidth. The results reported for **4** are corrected for this 2PF contribution.

The structure–property relationships in this initial library of compounds provide insight into the design of the next generation of compounds with optimized second-order nonlinear optical properties. One point of interest is the effect of phosphite substitution on β. A comparison of the β values of the NLO chromophores with the corresponding phosphites (**1**; cf. **2/3**) shows that phosphite functionalization of the second-order NLO chromophores causes a small decrease in the β values. This is not surprising, because phosphites are electron-withdrawing, therefore a phosphite ester oxygen atom should be a poorer donor than a hydroxy oxygen atom. However, when NHA is compared with **4**, there is little change in the observed β. This indicates that the electron-withdrawing effect of the phosphite group is counteracted by the electron-withdrawing effect of the azo bridge. It is also interesting that the binaphthyl-derived phosphite **3** exhibits a smaller decrease in β than does the analogous biphenyl-derived phosphite **2**. The differences in the β values are likely due to the difference in the steric

bulk of the biphenyl- and binaphthyl-derived phosphites, because the two groups should have similar electron-withdrawing abilities.

It is also interesting to compare the β values for the *cis*-Mo(CO)₄L₂ complexes **5** and **7** with the predictions of a simple additive model for a Λ-shaped dimer composed of 1D chromophores (for which β_{zzz} is the only nonzero tensor component).[37] In the case that the angle between the chromophores is $\theta = 90°$, the model predicts that the nonzero tensor components for the dimer are $\beta_{zzz} = \beta_{zxx}$, the depolarization ratio is $I_{VV}/I_{HV} = 5$, and β_{HRS} for the dimer is 1.87-times β_{HRS} for the monomer. For ligands **2** and **3** the observed depolarization ratio 4.4 ± 0.2 is consistent with $\beta_{zxx}/\beta_{zzz} = -0.06$, so the assumed dominance of β_{zzz} for the free ligand is a good approximation, and the angle $\theta = 85.8(3)°$ from the X-ray crystal structure of **5** is close to $\theta = 90°$. Both the depolarization ratios (**5**: 4.6 ± 0.1; **7**: 4.2 ± 0.1) and the ratios of β_{HRS} for the dimer and monomer (**5**: 1.51 ± 0.08; **7**: 1.35 ± 0.07) for the complexes are smaller than the values predicted for $\theta = 90°$. Adjustment of the angle can force agreement for either the depolarization ratio (at $\theta \approx 100°$) or β_{HRS} (at $\theta \approx 125°$), but not both simultaneously. However, the dipole–induced-dipole interaction between the chromophores is expected to decrease β_{zzz} and leave β_{zxx} unchanged. Fixing the angle at $\theta = 86°$ and reducing the additive model β_{zzz} for the dimer by the factor A (**5**: 0.72; **7**: 0.58) gives agreement with all the observations. This suggests that the simple noninteracting model correctly predicts the large off-diagonal component β_{zxx}, but interaction between the chromophores reduces the diagonal component β_{zzz} for the complex.

Finally, the relationship between the β and λ_{max} values of the compounds is of interest. It can be used to predict the β values of similar compounds, and it also gives an indication of the trade-off between nonlinearity and transparency.[38] Transparency is highly desirable for these compounds; however, it must not compromise their nonlinearity. Figure 3 shows a logarithmic plot of β vs. λ_{max} for all compounds with the Schiff base chromophore (**1–3**, **5**, and
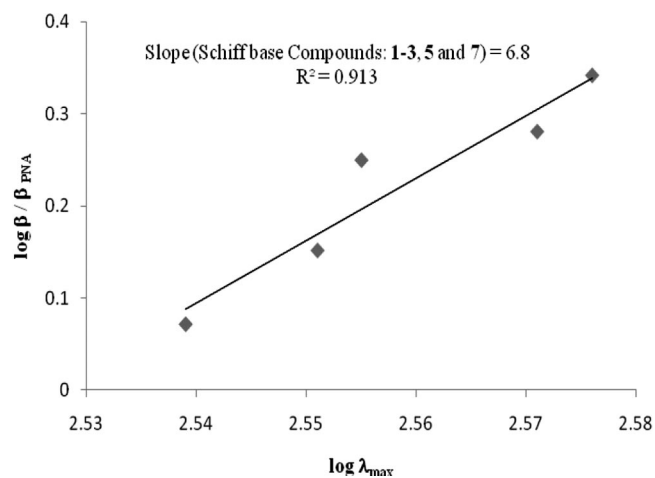
Figure 3. Plot of $\log\beta$ vs. $\log\lambda_{max}$ for Schiff base compounds **1–3**, **5**, and **7**.

7). There is a good correlation between $\log\beta$ and $\log\lambda_{max}$, with $\beta \propto \lambda_{max}{}^{6.8}$. NHA and compound **4** are diazo derivatives (different functional group) and therefore are not included in the correlation. The slope of the line in Figure 3 (6.8) is intermediate between the slopes similarly obtained for *para*-substituted benzenes (4.4) and stilbenes (8.7).[38]

Conclusions

We have developed a novel class of remarkably stable phosphite ligands with second-order NLO chromophores as substituents and their corresponding transition-metal complexes. The ligands have been prepared with phosphite groups. HRS measurements of the ligands in solution demonstrate that the second-order NLO properties of the ligands are primarily a function of the chromophores, but are also sensitive to the nature of the phosphite substituent. This demonstrates that modification of both the chromophore and the phosphite moiety can be used to improve the first hyperpolarizability (β) of the ligand. Modification of the phosphite substituent and the transition-metal center to which it is attached can also be used to orient the chromophores. A plot of $\log\beta$ vs. $\log\lambda_{max}$ shows a direct relationship between the two properties and also confirms the existence of a trade-off between the transparency and the nonlinearity of the compounds. We are currently exploring the use of phosphorus-based substituents on other known chromophores with better donor abilities.

Experimental Section

Materials and Methods: All manipulations were carried out under dry nitrogen by using standard Schlenk-line and glove-box techniques.[40] All solvents and NEt$_3$ were distilled from the appropriate drying agent and stored over molecular sieves (4 Å) under nitrogen until use. Unless otherwise stated, all reagents were obtained commercially and used without further purification. The 1,1′-biphenyl-2,2′-diol, (±)-1,1′-binaphthyl-2,2′-diol, and (–)-(*S*)-1,1′-binaphthyl-2,2′-diol, purchased from Aldrich, were dried by azeotropic distillation with toluene. The 1,1′-biphenyl-2,2′-diyl phosphorochloridite,[41] (±)-1,1′-binaphthyl-2,2′-diyl phosphorochloridite,[42] (–)-(*S*)-1,1′-binaphthyl-2,2′-diyl phosphorochloridite,[43] 4-hydroxy-4′-nitroazobenzene (NHA),[44] PdCl$_2$(MeCN)$_2$[45], and Mo(CO)$_4$(nbd)[46] were prepared according to literature methods.

Characterization: ^{31}P{^{1}H}, ^{13}C{^{1}H} and ^{1}H NMR spectra were recorded with a Bruker DRX400 FT-NMR spectrometer with 85% H$_3$PO$_4$ and (CH$_3$)$_4$Si as external and internal references, respectively. Chemical shifts (δ) are in parts per million (ppm). Elemental analyses were performed by Atlantic Microlab, Inc.

4-{[(4-Nitrophenyl)methylene]amino}phenol, O$_2$N-1-C$_6$H$_4$-4-CH=N-1-C$_6$H$_4$-4-OH (1): The synthesis and purification of **1** was adapted from literature methods that have been used to prepare related compounds.[47,48] A solution of 4-nitrobenzaldehyde (3.00 g, 20.0 mmol) in MeCN (50 mL) was added slowly to a stirred solution of 4-aminophenol (2.20 g, 20.0 mmol) in MeOH (50 mL) at room temperature. The reaction mixture was stirred for 2 h, until a bright orange color was observed. The bright orange solution was then concentrated to dryness at 50 °C under aspirator vacuum, and the solid residue was recrystallized from hot toluene to give

4.07 g (84.5%) of **1**. ^{1}H NMR (400 MHz, MeOD, 25 °C): δ = 8.65 (s, 1 H, C*H*=N), 8.29 (d, $^3J_{H,H}$ = 8.7 Hz, 2 H, C$_{Ar}$*H*), 8.07 (d, $^3J_{H,H}$ = 9.0 Hz, 2 H, C$_{Ar}$*H*), 7.26 (d, $^3J_{H,H}$ = 9.0 Hz, 2 H, C$_{Ar}$*H*), 6.83 (d, $^3J_{H,H}$ = 8.7 Hz, 2 H, C$_{Ar}$*H*) ppm. ^{13}C NMR (400 MHz, MeOD, 25 °C): δ = 157.63 (s, *C*H=N), 155.17 (s, *C$_{Ar}$*O), 129.17 (s, *C$_{Ar}$*H), 123.88 (s, *C$_{Ar}$*H), 123.01 (s, *C$_{Ar}$*H), 115.91 (s, *C$_{Ar}$*H) ppm. C$_{13}$H$_{10}$N$_2$O$_3$ (242.23): calcd. C 64.46, H 4.16; found C 64.44, H 4.14.

1,1′-Biphenyl-2,2′-diyl 4-{[(4-Nitrophenyl)methylene]amino}phenyl Phosphite, O$_2$N-1-C$_6$H$_4$-4-CH=N-1-C$_6$H$_4$-4-OP(OC$_6$H$_4$)$_2$ (2): A solution of 1,1′-biphenyl-2,2′-diyl phosphorochloridite (1.30 g, 5.20 mmol) in THF (7 mL) was added to a stirred mixture of 4-{[(4-nitrophenyl)methylene]amino}phenol (1.25 g, 5.20 mmol) and NEt$_3$ (0.73 mL, 5.20 mmol) in THF (20 mL) in a 100 mL Schlenk tube. The mixture was stirred at room temperature for 1 h during which time the triethylammonium chloride byproduct precipitated from the solution. The solution was separated from the precipitate by cannula filtration. The filtrate was then concentrated to dryness under reduced pressure. The residue was dissolved in dichloromethane (15 mL) and quickly filtered through a ca. 2 cm thick pad of silica gel in a 15 mL medium sintered glass funnel under nitrogen. The filtrate was then concentrated to dryness under reduced pressure to give a bright yellow solid. Recrystallization from CH$_2$Cl$_2$/hexanes by using a layering technique gave 2.06 g (89.3%) of **2** as yellow crystals. ^{31}P{^{1}H} NMR (400 MHz, CDCl$_3$, 25 °C): δ = 144.33 (s) ppm. ^{1}H NMR (400 MHz, CDCl$_3$, 25 °C): δ = 8.56 (s, 1 H, C*H*=N), 8.33 (d, $^3J_{H,H}$ = 8.8 Hz, 2 H, C$_{Ar}$*H*), 8.07 (d, $^3J_{H,H}$ = 8.8 Hz, 2 H, C$_{Ar}$*H*), 7.51 (dd, $^3J_{H,H}$ = 7.6, $^4J_{P,H}$ = 1.7 Hz, 2 H, C$_{Ar}$*H*), 7.42–7.22 (m, 10 H, C$_{Ar}$*H*) ppm. ^{13}C NMR (400 MHz, CDCl$_3$, 25 °C): δ = 157.16 (s, *C*H=N), 151.30 (d, $^2J_{P,C}$ = 7.3 Hz, *C$_{Ar}$*O), 149.66 (s, *C$_{Ar}$*NO$_2$), 149.26 (d, $^2J_{P,C}$ = 5.1 Hz, *C$_{Ar}$*O), 147.47 (s, *C$_{Ar}$*N=C), 141.95 (s, *C$_{Ar}$*CH=N), 131.50 (d, $^3J_{P,C}$ = 3.3 Hz, *C$_{Ar}$*C$_{Ar}$), 130.51 (s, *C$_{Ar}$*H), 129.78 (s, *C$_{Ar}$*H), 129.73 (s, *C$_{Ar}$*H), 126.04 (s, *C$_{Ar}$*H), 124.46 (s, *C$_{Ar}$*H), 122.91 (s, *C$_{Ar}$*H), 122.50 (d, |$^3J_{PC}$| = 1.3 Hz, *C$_{Ar}$*H), 121.72 (d, $^3J_{P,C}$ = 7.6 Hz, *C$_{Ar}$*H) ppm. C$_{25}$H$_{17}$N$_2$O$_5$P (456.39): calcd. C 65.79, H 3.75; found C 65.62, H 3.95.

(±)-1,1′-Binaphthyl-2,2′-diyl 4-{[(4-Nitrophenyl)methylene]amino}-phenyl Phosphite, O$_2$N-1-C$_6$H$_4$-4-CH=N-1-C$_6$H$_4$-4-OP(OC$_{10}$H$_6$)$_2$ (3): A solution of (±)-1,1′-binaphthyl-2,2′-diyl phosphorochloridite (1.21 g, 3.45 mmol) in THF (5 mL) was added to a stirred mixture of 4-{[(4-nitrophenyl)methylene]amino}phenol (0.83 g, 3.45 mmol) and NEt$_3$ (0.48 mL, 3.45 mmol) in THF (10 mL) in a 50 mL Schlenk tube. The mixture was stirred at room temperature for 2 h during which time the triethylammonium chloride byproduct precipitated from the solution. The solution was separated from the precipitate by cannula filtration. The filtrate was then concentrated to dryness under reduced pressure. The solid residue was redissolved in 15 mL of dichloromethane and filtered through a ca. 2 cm thick pad of silica gel in a 15 mL medium sintered glass funnel under nitrogen. Concentration to dryness under reduced pressure gave 1.28 g (67.0%) of pure **3** as a bright yellow solid. ^{31}P{^{1}H} NMR (400 MHz, CD$_2$Cl$_2$, 25 °C): δ = 145.71 (s) ppm. ^{1}H NMR (400 MHz, CD$_2$Cl$_2$, 25 °C): δ = 8.60 (s, 1 H, C*H*=N), 8.33 [d, ^3J(H,H) = 9.0 Hz, 2 H, C$_{Ar}$*H*], 8.10–7.97 (m, 6 H, C$_{Ar}$*H*), 7.62–7.20 (m, 12 H, C$_{Ar}$*H*) ppm. ^{13}C NMR (400 MHz, CD$_2$Cl$_2$, 25 °C): δ = 157.49 (s, *C*H=N), 151.16 (d, $^2J_{P,C}$ = 7.9 Hz, *C$_{Ar}$*O), 149.68 (s, *C$_{Ar}$*NO$_2$), 147.85 (d, $^2J_{P,C}$ = 4.4 Hz, *C$_{Ar}$*O), 147.71 (s, *C$_{Ar}$*N=C), 147.28 (d, $^2J_{P,C}$ = 2.3 Hz, *C$_{Ar}$*O), 142.05 (s, *C$_{Ar}$*CH=N), 133.15 (s, *C$_{Ar}$*H), 132.87 (s, *C$_{Ar}$*H), 132.18 (s, *C$_{Ar}$*H), 131.72 (s, *C$_{Ar}$*H), 131.07 (s, *C$_{Ar}$*H), 130.39 (s, *C$_{Ar}$*H), 129.75 (s, *C$_{Ar}$*H), 128.87 (s, *C$_{Ar}$*H), 128.79 (s, *C$_{Ar}$*H), 127.17 (s, *C$_{Ar}$*H), 127.10 (s, *C$_{Ar}$*H), 126.90 (s, *C$_{Ar}$*H), 126.81 (s, *C$_{Ar}$*H), 125.77 (s, *C$_{Ar}$*H), 125.61 (s, *C$_{Ar}$*H), 124.63

(s, C_{Ar}H), 124.36 (s, C_{Ar}H), 124.32 (s, C_{Ar}H), 122.96 (s, C_{Ar}H), 121.97 (s, C_{Ar}H), 121.59 (s, C_{Ar}H), 121.51 (s, C_{Ar}H) ppm. $C_{33}H_{21}N_2O_5P$ (556.51): calcd. C 71.22, H 3.80; found C 70.93, H 4.11.

(–)-4-Hydroxy-4′-nitroazophenyl (S)-1,1′-Binaphthyl-2,2′-diyl Phosphite, O_2N-1-C_6H_4-4-N=N-1-C_6H_4-4-OP$(OC_{10}H_6)_2$ (4): The procedure for **3** was repeated with a solution of (–)-(S)-1,1′-binaphthyl-2,2′-diyl phosphorochloridoite (0.69 g, 2.0 mmol) in THF (5 mL) and a mixture of 4-hydroxy-4′-nitroazobenzene (NHA) (0.48 g, 2.0 mmol) and NEt₃ (0.27 mL, 2.0 mmol) in THF (10 mL) to yield 0.54 g (50%) of pure **4** as a bright orange, microcrystalline solid. $^{31}P\{^1H\}$ NMR (400 MHz, CD_2Cl_2, 25 °C): δ = 145.02 (s) ppm. ^1H NMR (400 MHz, CD_2Cl_2, 25 °C): δ = 8.38 (d, $^3J_{H,H}$ = 8.9 Hz, 2 H, C_{Ar}H), 8.09–7.98 (m, 8 H, C_{Ar}H), 7.51–7.33 (m, 10 H, C_{Ar}H) ppm. $C_{32.1}H_{20.2}Cl_{0.2}N_3O_5P$ (4·0.1CH₂Cl₂) (565.99): calcd. C 68.11, H 3.60; found: C 67.94, H 3.59.

Tetracarbonyl(1,1′-biphenyl-2,2′-diyl 4-{[(4-nitrophenyl)methylene]amino}phenyl phosphite)molybdenum(0), cis-Mo(CO)₄(2)₂ (5): Solutions of **2** (0.20 g, 0.45 mmol) in CH_2Cl_2 (5 mL) and Mo(CO)₄-(nbd) (0.07 g, 0.2 mmol) in CH_2Cl_2 (5 mL) were added simultaneously and dropwise to a 100 mL Schlenk flask equipped with a stirrer bar. The solution was stirred at room temperature for 3 h. The orange-yellow solution was then concentrated under reduced pressure, and the solid residue was triturated with hexanes. Recrystallization by layering hexanes on a CH_2Cl_2 solution of the solid residue gave 0.17 g (70%) of pure **5** as orange-yellow crystals. $^{31}P\{^1H\}$ NMR (400 MHz, CD_2Cl_2, 25 °C): δ = 174.84 (s) ppm. ^1H NMR (400 MHz, CD_2Cl_2, 25 °C): δ = 8.39 (s, 2 H, CH=N), 8.24 (d, $^3J_{H,H}$ = 8.9 Hz, 4 H, C_{Ar}H), 7.99 (d, $^3J_{H,H}$ = 8.8 Hz, 4 H, C_{Ar}H), 7.45 (dd, $^3J_{H,H}$ = 8.0, $^4J_{H,H}$ = 1.9 Hz, 4 H, C_{Ar}H), 7.32–7.05 (m, 20 H, C_{Ar}H) ppm. ^{13}C NMR (400 MHz, CD_2Cl_2, 25 °C): δ = 210.62 (m, AXX′, trans-CO), 205.62 (m, AX₂, cis-CO), 157.58 (s, CH=N), 150.86 (s, C_{Ar}O), 149.69 (s, C_{Ar}NO₂), 149.64 (s, C_{Ar}O), 148.14 (s, C_{Ar}N=C), 141.98 (s, C_{Ar}CH=N), 130.64 (s, $C_{Ar}C_{Ar}$), 130.47 (s, C_{Ar}H), 129.89 (s, C_{Ar}H), 129.76 (s, C_{Ar}H), 126.29 (s, C_{Ar}H), 124.35 (s, C_{Ar}H), 122.68 (s, C_{Ar}H), 122.63 (s, C_{Ar}H), 122.58 (s, C_{Ar}H) ppm. $C_{54}H_{34}MoN_4O_{14}P_2$ (1120.76): calcd. C 57.87, H 3.06; found C 57.46, H 3.00.

(1,1′-Biphenyl-2,2-diyl 4-{[(4-nitrophenyl)methylene]amino}phenyl phosphite)dichloridopalladium(II), PdCl₂(2)₂ (6): Ligand **2** (0.043 g, 0.097 mmol) was added to a stirred solution of PdCl₂(MeCN)₂ (0.0085 g, 0.049 mmol) in CH_3CN (20 mL). A pale yellow precipitate was observed after stirring for 10 min. The reaction mixture was stirred for an additional 30 min. The solid was allowed to settle to the bottom of the flask, and the supernatant removed with a Pasteur pipette. The residue was washed with hexanes and dried under vacuum overnight to yield 0.051 g (>99%) of pure **6** as a pale yellow solid. $^{31}P\{^1H\}$ NMR (400 MHz, [D₆]DMSO, 25 °C): δ = 109.34 (s) ppm. ^1H NMR (400 MHz, [D₆]DMSO, 25 °C): δ = 8.68 (s, 2 H, CH=N), 8.31 (d, $^3J_{H,H}$ = 8.6 Hz, 2 H, C_{Ar}H), 8.16 (d, $^3J_{H,H}$ = 8.6 Hz, 4 H, C_{Ar}H), 7.62 (d, $^3J_{H,H}$ = 7.1 Hz, C_{Ar}H), 7.50–7.05 (m, 20 H, C_{Ar}H) ppm. ^{13}C NMR (400 MHz, [D₆]DMSO, 25 °C): δ = 160.20 (s, CH=N), 149.73 (s, C_{Ar}O), 149.10 (s, C_{Ar}NO₂), 148.10 (s, C_{Ar}O), 147.60 (s, C_{Ar}N=C), 142.13 (s, C_{Ar}CH=N), 131.52 (s, $C_{Ar}C_{Ar}$), 130.57 (s, C_{Ar}H), 129.04 (s, C_{Ar}H), 128.32 (s, C_{Ar}H), 124.90 (s, C_{Ar}H), 123.75 (s, C_{Ar}H), 122.56 (s, C_{Ar}H), 122.39 (s, C_{Ar}H), 121.58 (s, C_{Ar}H) ppm. $C_{50}H_{34}Cl_2N_4O_{10}P_2Pd$ (1090.11): calcd. C 55.09, H 3.14; found C 55.10, H 3.18.

[(–)-(S)-1,1′-Binathyl-2,2′-diyl 4-{[(4-nitrophenyl)methylene]amino}phenyl phosphite]tetracarbonylmolybdenum(0), cis-Mo(CO)₄-(3)₂ (7): Solutions of **3** (0.25 g, 0.45 mmol) in CH_2Cl_2 (5 mL) and Mo(CO)₄(nbd) (0.07 g, 0.2 mmol) in CH_2Cl_2 (5 mL) were added

simultaneously and dropwise to a 100-mL Schlenk flask equipped with a stirrer bar. The solution was stirred at room temperature for 7 h. The orange-yellow solution was then concentrated under reduced pressure, and the solid residue was triturated with hexanes. Recrystallization by layering hexanes on a CH_2Cl_2 solution of the solid residue gave 0.07 g (50%) of pure **7** as an orange-yellow microcrystalline solid. $^{31}P\{^1H\}$ NMR (400 MHz, CD_2Cl_2, 25 °C): δ = 178.57 (s) ppm. ^1H NMR (400 MHz, CD_2Cl_2, 25 °C): δ = 8.32 (d, $^3J_{H,H}$ = 8.8 Hz, 4 H, C_{Ar}H), 8.24 (s, 2 H, CH=N), 8.00–7.90 (m, 10 H, C_{Ar}H), 7.77 (d, $^3J_{H,H}$ = 8.9 Hz, 2 H, C_{Ar}H), 7.58 (d, $^3J_{H,H}$ = 8.8 Hz, 2 H, C_{Ar}H), 7.50–7.25 (m, 14 H, C_{Ar}H), 7.03 (d, $^3J_{H,H}$ = 8.7 Hz, 4 H, C_{Ar}H), 6.84 (dd, $^3J_{H,H}$ = 8.8, $^4J_{H,H}$ = 1.9 Hz, 4 H, C_{Ar}H) ppm. ^{13}C NMR (400 MHz, CD_2Cl_2, 25 °C): δ = 157.17 (s, CH=N), 150.40 (s, C_{Ar}O), 149.28 (s, C_{Ar}NO₂), 148.59 (s, C_{Ar}O), 147.76 (s, C_{Ar}N=C), 147.08 (s, C_{Ar}O), 141.57 (s, C_{Ar}CH=N), 132.84 (s, C_{Ar}H), 132.32 (s, C_{Ar}H), 131.71 (s, C_{Ar}H), 131.21 (s, C_{Ar}H), 130.50 (s, C_{Ar}H), 129.95 (s, C_{Ar}H), 129.32 (s, C_{Ar}H), 129.32 (s, C_{Ar}H), 128.27 (s, C_{Ar}H), 127.04 (s, C_{Ar}H), 126.80 (s, C_{Ar}H), 126.40 (s, C_{Ar}H), 126.36 (s, C_{Ar}H), 125.40 (s, C_{Ar}H), 125.34 (s, C_{Ar}H), 123.95 (s, C_{Ar}H), 122.98 (s, C_{Ar}H), 122.80 (s, C_{Ar}H), 122.47 (s, C_{Ar}H), 122.17 (s, C_{Ar}H), 122.06 (s, C_{Ar}H), 121.01 (s, C_{Ar}H) ppm. $C_{72.4}H_{46.8}MoN_4O_{14}P_2$ (7·0.5C₆H₁₂) (1354.67): calcd. C 64.19, H 3.48; found: C 64.47, H 3.52.

X-ray Data Collection and Solution: Suitable single crystals of **2** and **5** were glued on glass fibers with epoxy and aligned upon an Enraf–Nonius CAD4 single-crystal diffractometer under aerobic conditions. Standard peak search and automatic indexing routines followed by least-squares fits of 25 accurately centered reflections resulted in accurate unit cell parameters for each. The space groups of the crystals were assigned on the basis of systematic absences and intensity statistics. All data collections were carried out by using the CAD4-PC software,[49] and details of the data collections are given in Table 5. The analytical scattering factors of the complex were corrected for both $\Delta f'$ and $i\Delta f''$ components of anomalous dispersion. All data were corrected for Lorentz and polarization effects. The data for compound **5** were corrected for absorption by using ψ-scans of four reflections with χ > 80°, and empirical absorption corrections were applied when necessary. All crystallographic calculations were performed with the Siemens SHELXTL-PC program package.[50] The Mo and P positions were located by using the Patterson method with all non-hydrogen atoms located in difference Fourier maps. Full-matrix refinements of the positional and anisotropic thermal parameters for all non-hydrogen atoms vs. F^2 were carried out. All hydrogen atoms were placed in calculated positions with the appropriate molecular geometry and δ(C–H) = 0.93 Å for aromatic hydrogen atoms. The isotropic thermal parameter of each hydrogen atom was fixed equal to 1.2-times the U_{eq} value of the atom to which it is bound. Selected torsion angles, bond angles, and bond lengths for **2** and **5** are given in Tables 1, 2, and 3, respectively. The dihedral angle between the ligands in compound **5** was found to be 85.8(3)°. CCDC-750122 (for **2**) and -750123 (for **5**) contain the crystallographic data for this paper. These data can be obtained free of charge from The Cambridge Crystallographic Data Centre via www.ccdc.cam.ac.uk/data_request/cif.

Linear and Nonlinear Optical Characterization: The linear optical properties of the ligands in solution were characterized by UV/Vis spectroscopy. Electronic spectra were recorded of 1.0×10^{-5} M solutions of the ligands and complexes in 1,4-dioxane with a Varian Cary-100 UV/Vis spectrophotometer. The experimental methods used for the HRS measurements were similar to those previously reported.[32,51] Linearly polarized pulses (1064 nm wavelength, 35 μJ pulse energy, 100 ns pulse duration, 4 kHz repetition rate)

Table 5. Crystal data and structure refinement for **2** and **5**.

	2	**5**
Empirical formula	$C_{25}H_{17}N_2O_5P$	$C_{54}H_{34}MoN_4O_{14}P_2$
Formula mass	456.38	1120.73
Temperature [K]	293(2)	293(2)
Wavelength [Å]	0.71073	0.71073
Crystal system	monoclinic	monoclinic
Space group	$P2_1/c$	$P2_1/n$
a [Å]	9.910(2)	10.697(2)
b [Å]	28.093(6)	35.989(7)
c [Å]	7.8199(16)	13.090(3)
β [°]	101.08(3)	92.51(3)
Volume [Å^3]	2136.6(7)	5034.7(17)
Z	4	4
Density (calculated) [Mg/m^3]	1.419	1.479
Absorption coefficient μ [mm^{-1}]	0.170	0.397
$F(000)$	944	2280
Crystal size [mm]	$0.4 \times 0.6 \times 0.8$	$0.2 \times 0.4 \times 0.8$
θ range for data collection [°]	2.09–22.48	2.22–22.47
Index ranges	$-10 \leq h \leq 10$	$-1 \leq h \leq 11$
	$30 \leq k \leq 30$	$0 \leq k \leq 38$
	$-8 \leq l \leq 1$	$-14 \leq l \leq 14$
Reflections collected	6932	7810
Independent reflections	2794 [R(int) = 0.0759]	6559 [R(int) = 0.0593]
Completeness to $\theta = 22.48°$	100.0%	99.9%
Absorption correction	none	empirical
Max./min. transmission	–	0.2608/0.2362
Refinement method	full-matrix least squares on F^2	full-matrix least squares on F^2
Data/restraints/parameters	2794/0/298	6559/0/676
Goodness-of-fit on F^2	1.106	0.964
Final R indices [$I > 2\sigma(I)$]	R1 = 0.0658, wR2 = 0.1637	R1 = 0.0640, wR2 = 0.1530
R indices (all data)	R1 = 0.1026, wR2 = 0.1809	R1 = 0. 1801, wR2 = 0.1953
Largest difference peak/hole [eÅ^{-3}]	0.489/–0.341	0.655/–0.507

from an injection-seeded single-longitudinal-mode Nd:YAG (yttrium aluminum garnet) laser were focused into the liquid sample (6 µm beam waist diameter) contained in a 1 cm spectroscopic cuvette. Light scattered around the 90° scattering angle was collected and collimated by a numerical aperture 0.62 lens, analyzed by a polarizing beam splitter, and then fiber-coupled to an interference filter (532 nm peak, 60 cm^{-1} bandwidth) and the photon counting detector. A fiber-coupled dual etalon filter was inserted to narrow the bandwidth to 0.3 cm^{-1}. Samples were 6 mM solutions of the compounds in 1,4-dioxane that were filtered through a 0.2 µm micropore filter. Measurements were calibrated by using a 90 mM solution of 4-nitroaniline (pNA) in 1,4-dioxane (β = 21.3×10^{-30} esu) as the reference. The β values were obtained from HRS measurements in the VV polarization geometry.

Acknowledgments

[1] A. Dulcic, *Chem. Phys.* **1979**, *37*, 57–61.

[2] D. F. Eaton, *Science* **1991**, *253*, 281–287 and references therein.

[3] M. Burland, *Chem. Rev.* **1994**, *94*, 1–278.

[4] T. J. Marks, M. A. Ratner, *Angew. Chem. Int. Ed. Engl.* **1995**, *34*, 155–173.

[5] I. Ledoux, J. Zyss, E. Barni, C. Barolo, N. Diulgheroff, P. Quagliotto, *Synth. Met.* **2000**, *115*, 213–217.

[6] Y. D. Zhang, L. M. Wang, T. Wada, H. Sasabe, *Macromolecules* **1996**, *29*, 1569–1573.

[7] R. Burzynski, M. K. Cassterens, Y. Zhang, *Opt. Eng.* **1996**, *35*, 443–451.

[8] S. K. Yesodha, C. K. Sadahiva Pillai, N. Jsutsumi, *Prog. Polym. Sci.* **2004**, *29*, 45–74.

[9] M. Jazbinsek, P. Gunter, *Opt. Sci. Eng.* **2008**, *133*, 421–466.

[10] K. Yu. Suponitsky, T. V. Timofeeva, M. Yu. Antipin, *Russ. Chem. Rev.* **2006**, *75*, 457–496.

[11] G. Yang, Z. Su, C. Qin, *J. Phys. Chem. A* **2006**, *110*, 4817–4821.

[12] S. Debrus, H. Ratajczak, J. Venturini, N. Pincon, J. Baran, J. Barycki, T. Glowiak, A. Pietraszko, *Synth. Met.* **2002**, *127*, 99–104.

[13] E. Goovaerts, W. E. Wenseleers, M. H. Garcia, G. H. Cross in *Handbook of Advanced Electronic and Photonic Materials and Devices* (Ed.: H. S. Nalwa), Academic Press, New York, **2001**, vol. 9, pp. 127–191.

[14] S. Houbrechts, E. Hendrickx, T. Verbiest, K. Clays, A. Persoons, V. Balzani, *Adv. Electron Transfer Chem.* **2001**, *5*, 243–281.

[15] J.-B. Gaudry, L. Capes, P. Langot, S. Marcen, M. Kollmannsberger, O. Lavastre, E. Freysz, J.-F. Letard, O. Kahn, *Chem. Phys. Lett.* **2000**, *324*, 321–329.

[16] S. R. Marder, D. N. Beratan, B. G. Tiemann, L. T. Cheng, W. Tam, *Spec. Publ. R. Soc. Chem.* **1991**, *91*, 165–175.

[17] H. E. Katz, C. W. Dirk, K. D. Singer, J. E. Sohn, *Mol. Cryst. Liq. Cryst.* **1988**, *157*, 525–533.

[18] H. E. Katz, K. D. Singer, J. E. Sohn, C. W. Dirk, L. A. King, H. M. Gordon, *J. Am. Chem. Soc.* **1987**, *109*, 6561–6563.

[19] T. Rasing, G. Berkovic, Y. R. Shen, S. G. Grubb, M. W. Kim, *Chem. Phys. Lett.* **1986**, *130*, 1–5.

[20] a) L. Sanguinet, J.-L. Pozzo, V. Rodriguez, F. Adamietz, F. Castet, L. Ducasse, B. Champagne, *J. Phys. Chem. B* **2005**, *109*, 11139–11150; b) F. Mancois, J.-L. Pozzo, J. Pan, F. Adamietz,

V. Rodriguez, L. Ducasse, F. Castet, A. Plaquet, B. Champagne, *Chem. Eur. J.* **2009**, *15*, 2560–2571.

[21] C.-G. Liu, Y.-Q. Qiu, S.-L. Sun, N. Li, G.-C. Yang, Z.-M. Su, *Chem. Phys. Lett.* **2007**, *443*, 163–168.

[22] H. Unver, A. Elmali, A. Karakas, H. Kara, E. Donmez, *J. Mol. Struct.* **2006**, *800*, 18–22.

[23] Z.-M. Xue, Y.-W. Tang, J.-Y. Wu, Y.-P. Tian, M.-H. Jiang, H.-K. Fun, A. Usman, *Can. J. Chem.* **2004**, *82*, 1700–1706.

[24] J. Costes, J. Lamere, C. Lepetit, P. G. Lacroix, F. Dahan, K. Nakatani, *Inorg. Chem.* **2005**, *44*, 1973–1982.

[25] a) I. Sheikhshoaie, M. Hossein, S. Saeid-Nia, *J. Coord. Chem.* **2004**, *57*, 417–423; b) F. Cariati, U. Caruso, R. Centore, A. De Maria, M. Fusco, B. Panunzi, A. Roviello, A. Tuzi, *Inorg. Chim. Acta* **2004**, *357*, 548–556.

[26] S. Di Bella, C. Dragonetti, M. Pizzotti, D. Roberto, F. Tessore, R. Ugo, *Top. Organomet. Chem.* **2010**, *28*, 1–55.

[27] H. Byrd, J. D. Harden, J. M. Butler, M. J. Jablonsky, G. M. Gray, *Organometallics* **2003**, *22*, 4198–4205.

[28] G. M. Gray, F. P. Fish, D. K. Srivastava, A. Varshney, M. J. van der Woerd, S. E. Ealick, *J. Organomet. Chem.* **1990**, *385*, 49–60.

[29] R. D. Myrex, C. S. Colbert, G. M. Gray, *Organometallics* **2004**, *23*, 409–415.

[30] J. Liu, R. S. Loewe, R. D. McCullough, *Macromolecules* **1999**, *32*, 5777–5785.

[31] S. J. Lee, J. S. Kim, W. Lin, *Inorg. Chem.* **2004**, *43*, 6579–6588.

[32] a) M. Stahelin, D. M. Burland, J. E. Rice, *Chem. Phys. Lett.* **1992**, *191*, 245–250; b) P. Kaatz, D. P. Shelton, *J. Chem. Phys.* **1996**, *105*, 3918–3929.

[33] P. Kaatz, E. A. Donley, D. P. Shelton, *J. Chem. Phys.* **1998**, *108*, 849–856.

[34] J. L. Oudar, D. S. Chemla, *J. Chem. Phys.* **1977**, *66*, 2664–2668.

[35] a) J. Zyss, *J. Chem. Phys.* **1979**, *70*, 3333–3340; b) J. Zyss, *J. Chem. Phys.* **1979**, *70*, 3341–3349; c) J. Zyss, *J. Chem. Phys.* **1979**, *71*, 909–916; d) D. S. Chemla, J. Zyss (Eds.), *Nonlinear Optical Properties of Organic Molecules and Crystals*, Academic Press, New York, **1987**.

[36] J. Campo, F. Desmet, W. Wenseleers, E. Goovaerts, *Opt. Express* **2009**, *17*, 4587–4604.

[37] K. Clays, A. Persoons, *J. Mol. Struct.* **2000**, *521*, 303–313.

[38] L.-T. Cheng, W. Tam, S. H. Stevenson, G. R. Meredith, *J. Phys. Chem.* **1991**, *95*, 10631–10643.

[39] M. N. Burnett, C. K. Johnson, *ORTEP-III, Oak Ridge Thermal Ellipsoid Plot Program for Crystal Structure Illustrations*, Oak Ridge National Laboratory Report ORNL-6895, **1996**.

[40] S. Komiya, K. Tatsumi, T. Mashima, T. Ito, M. Hurano, A. Fukuoka, F. Ozawa, K. Maruoka, N. Miyaura, T. Takeda, "Manipulation of Air-sensitive Compounds" in *Synthesis of Organometallic Compounds* (Ed.: S. Komiya), 1st ed., John Wiley and Sons Inc., New York, NY, **1998**, pp. 35–55.

[41] L. V. Verizhnikov, P. A. Kirpichnikov, *Zh. Obshch. Khim.* **1966**, *36*, 1355–1358.

[42] a) M. A. Brammer, W-J. Peng, J. M. Maher, WO 2008124468, **2008**; b) S. D. Pastor, S. P. Shum, US 5,391,799, **2008**.

[43] C. R. Smith, T. V. Rajanbabu, *Org. Lett.* **2008**, *10*, 1657–1659.

[44] Y. Cui, M. Wang, L. Chen, G. Qian, *Dyes Pigm.* **2005**, *65*, 61–66.

[45] a) I. Abrunhosa, L. Delain-Biotin, A.-C. Gaumont, M. Gulea, S. Masson, *Tetrahedron* **2004**, *60*, 9263–9272; b) M. Noskowska, E. Sliwinska, W. Duczmal, *Trans. Met. Chem.* **2003**, *28*, 756–759; c) M. A. Andres, T. C. T. Chang, C. W. F. Cheng, L. V. Kapustay, K. P. Kelly, M. J. Zweifel, *Organometallics* **1984**, *3*, 1479–1484.

[46] W. Ehrl, R. Ruck, H. J. Vahrenkamp, *Organomet. Chem.* **1973**, *56*, 285–293.

[47] a) D.-Y. Yang, Y.-S. Chen, P.-Y. Kuo, J.-T. Lai, C.-M. Jiang, C.-H. Lai, Y.-H. Liao, P.-T. Chou, *Org. Lett.* **2007**, *9*, 5287–5290; b) A. Iqbal, H. L. Siddiqui, C. M. Ashraf, M. H. Bukhari, C. M. Akram, *Chem. Pharm. Bull.* **2007**, *55*, 1070–1072.

[48] H. Neuvonen, K. Neuvonen, F. J. Fueloep, *J. Org. Chem.* **2006**, *71*, 3141–3148.

[49] *CAD4-PC Version 1.2*, Enraf–Nonius, Delft, The Netherlands, **1988**.

[50] G. M. Sheldrick, *SHELXTL NT Version 6.12*, Bruker AXS, Inc., Madison, WI, **2001**.

[51] D. P. Shelton, *J. Chem. Phys.* **2010**, *132*, 154506/1–154506/8.